Prace Instytutu Mechaniki Górotworu PAN
Tom 20, nr 2, Czerwiec 2018, s. 111-122

Modern applications of the Knothe theory in calculations of surface and rock mass deformations

Anton Sroka, Rafał Misa, Krzysztof Tajduś

Instytut Mechaniki Górotworu PAN; ul. Reymonta 27, 30-059 Kraków

Abstract

The theory of professor Stanisław Knothe has become a basis for practical prognostic calculations of mining impacts and, by the same token, it has allowed initiation of large scale exploitation of major coal, salt and metal ore deposits located in the protective pillars of towns and important surface constructions/facilities. The theory of professor Knothe is being successfully applied by the Polish and international mining industries for over sixty years. One can certainly say that it is one of the best known and internationally recognized achievements of the Polish mining science. The article presents a brief summary of contemporary applications of the Knothe theory in calculation of rock mass and surface subsidence not only in their classic form relevant to calculations for mining coal deposits. The solution presented here is based on a mathematical model of deposit impacts and it includes, among other things, subsidence caused by fluid deposit exploitation, heat extraction in deep geothermal applications and the uplifting of land surface caused by changes in mining water levels in closed hard coal mines.

Keywords: Knothe's theory, salt caverns, fluidized bed exploitation, reservoir mines, tunnels, deep geothermal installations

1. Introduction

The article will present a generalization of the Knothe theory consisting of an analysis of the deposit element impacts.

The size of the deposit element is determined in a way, so the trough formed by the extraction of this element is practically matching the fundamental solution in the form of a Gaussian function. Such a solution allows, among other things, precise consideration of the three-dimensional geometry of the selected deposit, i.e. the variation in its thickness and depth, inclination of the overlaying rock mass (overburden), its anisotropy, course of the mining operations in time through exact registration of the time of extraction of the deposit element and of other necessary information such as for example distribution of porosity and pressure in the case of fluid deposit exploitation (Sroka, 1984; Sroka, Schober, Bartosik-Sroka, 1988; Hejmanowski et al., 2001). The general diagram of the correlations is shown in figure 1.

To better understand the concept of calculations and their generalization to other domains of mining, a dual-consequence diagram has been used.

The causes include human mining activity related to the extraction of solid, liquid and gaseous raw materials, construction of caverns for oil and gas storage, extraction of „heat" from geothermal resources or the flooding of mines by increasing mining water level and the occurrence of disintegrated rock mass areas formed by earlier mining operations.

Consequence No. 1 is the convergence of an emptied cavity within the deposit element caused by longwall extraction of hard coal, room and pillar exploitation of sulphur deposits or metal ores, compaction of porous fluid deposits caused by reduction in the porous pressure, convergence of salt caverns, change in volume caused by cooling of the rock mass part due to extraction of „heat" or vertical expansion („decompaction") of disintegrated porous post-mining areas due to an increase of porous pressure resulting from increased levels of mining waters. Consequence No. 2 is the deformation of rock mass and land surface.

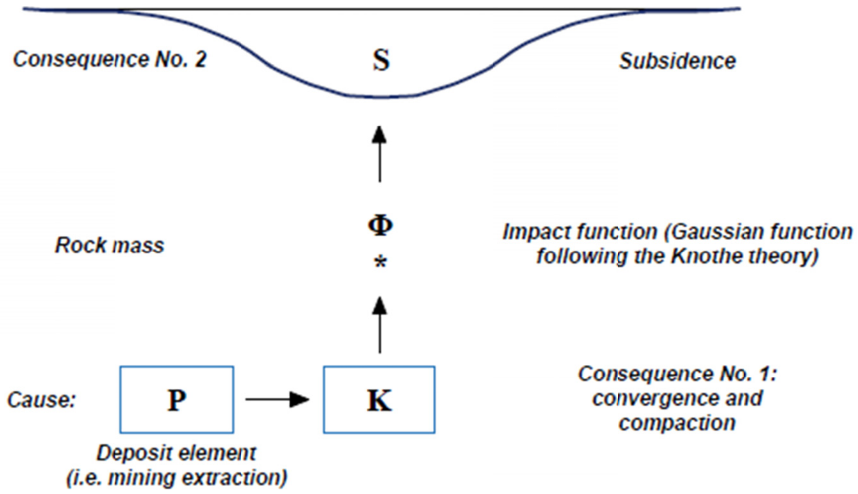

Fig. 1. Block diagram of the calculation model

Assuming that the impact function takes the form of a Gaussian function, with parameters given by Knothe (1951), we obtain (1):

$$s(r,t) = \frac{a \cdot K(t-\Delta t)}{R^2} \exp\left(-\pi \frac{r^2}{R^2}\right) \tag{1}$$

where:

- a – subsidence coefficient, depending on the mining method, being the ratio between the volume of the expected subsidence trough and the change in deposit zone volume caused by i.e. convergence or compaction (consequence No. 1),
- r – distance between the calculation point and the deposit element,
- $K(t)$ – change in deposit element volume in time t,
- R – radius of the main influences range ($R = H \cdot \cot\beta$),
- H – mining depth,
- β – angle of the main influences (Knothe, 1953),
- Δt – delay time caused by the retarding impact of the overlaying rock mass.

2. Calculation of land surface subsidence over salt cavern fields used for storage of liquid and gaseous energy resources

In the mid-eighties, land surface subsidence caused by convergence of caverns in salt rock mass in Germany has reached measurable values. In a project financed by the Lower Saxony government, based on the Knothe theory, Sroka and Schober (1982) have formulated a solution (2) for the distribution of subsidence over a single cavern (Fig. 2).

$$S(r,t) = s_{\max}(t) \cdot \frac{R_o \cdot R_u}{r \cdot h} \cdot \tan\beta \cdot \left[F\left(\frac{r}{R_u}\right) - F\left(\frac{r}{R_o}\right) \right] \tag{2}$$

$$F\left(\frac{r}{R}\right) = \int_{\frac{r}{R}}^{\infty} \exp\left(-\pi\lambda^2\right) d\lambda \tag{3}$$

where:

$$R_u = H_u \cdot \cot\beta, \qquad R_o = H_o \cdot \cot\beta, \tag{4}$$

- $S(r,t)$ – subsidence of a surface point at time t, point located on land surface in distance r from the axis of the cavern,
- $S_{\max}(t)$ – maximum subsidence at time t,

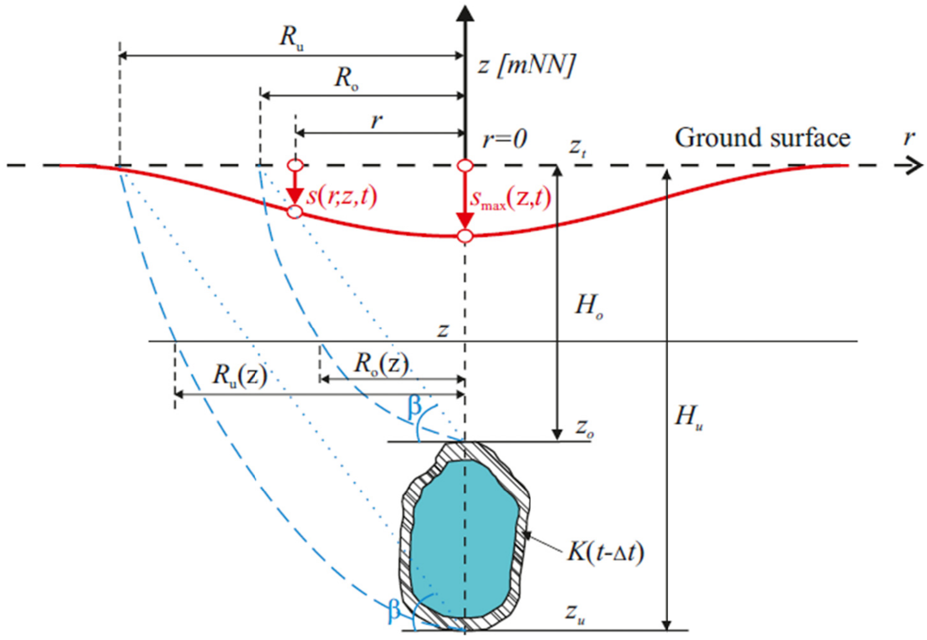

Fig. 2. Subsidence trough over a salt cavern

H_o – depth of the cavern roof,
H_u – depth of the cavern floor,
R_o – parameter of the horizontal influence scale in the horizontal direction (so-called radius of main influences, counted from the cavern roof),
R_u – radius of main influences, counted from the cavern floor,
h – height of the cavern.

Making a few simplifying assumptions, formula (2) can be replaced (with very good approximation) with formula (5):

$$S(r,t) = S_{\max}(t) \cdot \exp\left(-\pi \frac{r^2}{R^2}\right) \tag{5}$$

where:

$$R = \sqrt{R_o \cdot R_u} \tag{6}$$

Formula (5) indicates that there is a relationship between the maximum subsidence and the volume of the subsidence trough (7):

$$M(t) = S_{\max}(t) \cdot R^2,\; S_{\max} = \frac{M(t)}{R^2} \tag{7}$$

where: $M(t)$ – volume of the subsidence trough.

In the case of a cavern field, calculation of subsidence in a randomly selected point of the land surface is done by assuming a linear superposition – summing up the subsidence of individual caverns. The volume of the subsidence trough $M(t)$ depends on the volumetric convergence $K(t)$, on the delaying impact of the overlaying rock mass and possible losses of volume related to the deformation of the rock mas overlay. Convergence in time can be analytically described using a logarithmic or exponential function (Sroka 1984; Schober, Sroka 1987 and others). For example, assuming a model of incremental salting-out, Schober and Sroka (1987) concluded that the volume of the subsidence trough on the surface can be described by the following formula (8):

$$M(t) = a \cdot V \cdot \left(1 + \frac{f}{\xi - f} \cdot \exp(-\xi \cdot t) - \frac{\xi}{\xi - f} \cdot \exp(-f \cdot t)\right) \tag{8}$$

where:

- a – volume loss coefficient (a = 1.0 – passage across the rock mass without loss of volume),
- V – initial volume of the cavern,
- ξ – relative rate of volumetric convergence (i.e. $\xi = 0.02$ year^{-1} means that the volumetric convergence is taking place at a rate of 2% of the current volume per year),
- f – relative velocity of the trough's migration across the rock mass [year^{-1}].

In situ analyses of subsidence results indicate that coefficient a is practically equal to one, which means that there are no volume losses in the rock mass (Hartmann 1984; Sroka et al. 1987).

Formula (8) can be presented in a simplified form (9):

$$M(t) = a \cdot K(t - \Delta t) \tag{9}$$

$$\Delta t \approx \frac{\xi + f}{\xi \cdot f} \tag{10}$$

where:

- $K(t - \Delta t)$ – volumetric convergence of the cavern in time $t - \Delta t$,
- Δt – delay time caused by the retarding impact of the overlaying rock mass.

Value $S_{max}(t)$ also depends on the shape of the cavern (i.e. cylinder, sphere or cone) and on the geometric model of convergence (Haupt et al., 1983; Hartmann, 1984; Sroka et al., 2017 and others). Results of the comparative calculations performed lead to the conclusion that the value of maximum subsidence can be very well approximated with formula (11):

$$S_{max}(t) = \frac{a \cdot K(t - \Delta t)}{R^2} \tag{11}$$

Despite the necessary geometric and physical idealizations of cavern geometries, course of the convergence processes and phases of exploitation, the comparative calculations performed for the EPE cavern field (in Germany) have fully confirmed the suitability of the solution presented (Hengst 2014). Figure 3 shows a comparison of the subsidence values calculated and measured over the EPE cavern field.

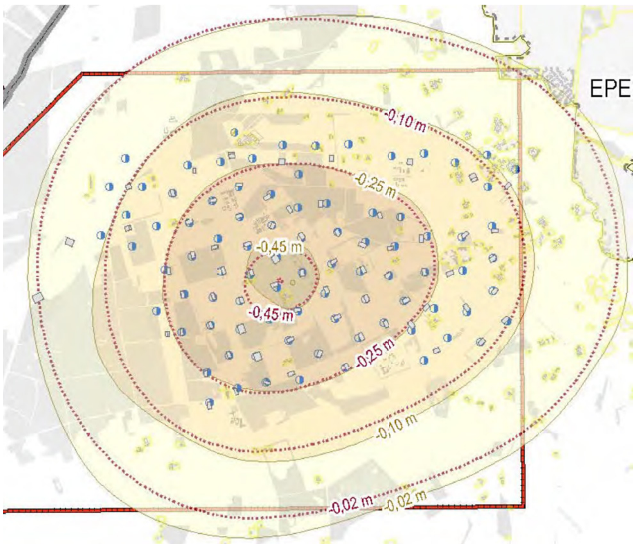

Fig. 3. Comparison of the 2006 subsidence measurement results (continuous line) and theoretical calculation results (dotted line) at the EPE cavern field (Hengst, 2014)

Additional algorithms have been developed to allow calculation of cavern convergence based on land surface subsidence measurements (Sroka, 1984; Leitzke, Sroka, 1987). In 2015-2017, the Solvay company has contracted development of a new software allowing calculation of all deformation indexes for land surface and rock mass, including among other things expected deformations along boreholes connecting land surface with the cavern. In reality such boreholes may be damaged by cavern convergence and lead to environmental threats (Sroka et al., 2017).

3. Subsidence calculations in fluid deposit exploitation

Following the calculation procedure presented for elements of a fluid deposit, the corresponding elementary trough on land surface can be described with the following Knothe theory-based formula (1). In this case, parameter $K(t)$ describes the compaction volume of a porous element of a fluid deposit at time t.

The horizontal dimension of the square-shaped deposit element shall not exceed $L \leq 0.1R$ (Sroka, 1984). An important stage is the break-down of the exploited fluid deposit into elements having the following parameters:

- coordinates x,y,z,
- depth H,
- thickness of the deposit layer M,
- porosity η,
- rigidity module E_s,
- porous pressure at different moments in time $p(t)$.

Such a discretization of the deposit (Fig. 4) allows complete consideration of the three-dimensional shape of the deposit and spatial distributions of properties, necessary to perform the calculation process.

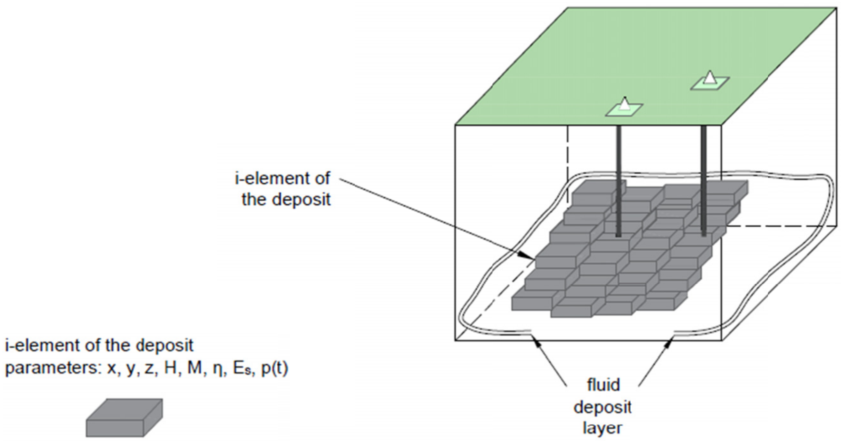

Fig. 4. Diagram of fluid deposit discretization to deposit elements

The cause-effect model indicates that the cause of land surface subsidence is the compaction of porous deposit rock formations due to a reduction in pore pressure. In the case of the deposit element (Fig. 5), deposit compaction leads to the formation of a so-called elementary trough, described with formula (12).

$$s_{j,i}(r,t) = \frac{\Delta M_i(t) \cdot L^2}{R_{j,i}^2} \exp\left(-\pi \frac{r_{j,i}^2}{R_{j,i}^2}\right) \tag{12}$$

where:

$\Delta M_i(t)$ – absolute vertical compaction of the i-element at time t,

$s_{j,i}(r,t)$ – subsidence of the j-point of land surface caused by compaction of the i-element of the deposit,

$r_{j,i}$ – distance between the j-calculation point and the i-element of the deposit.

Total subsidence of a random point of the land surface is being calculated with the assumption of the so-called linear superposition, which is the sum of point subsidence from individual elements of the deposit:

$$w_{j,i} = \sum_{i=1}^{i=N} w_{j,i} \tag{13}$$

where: N – number of deposit elements.

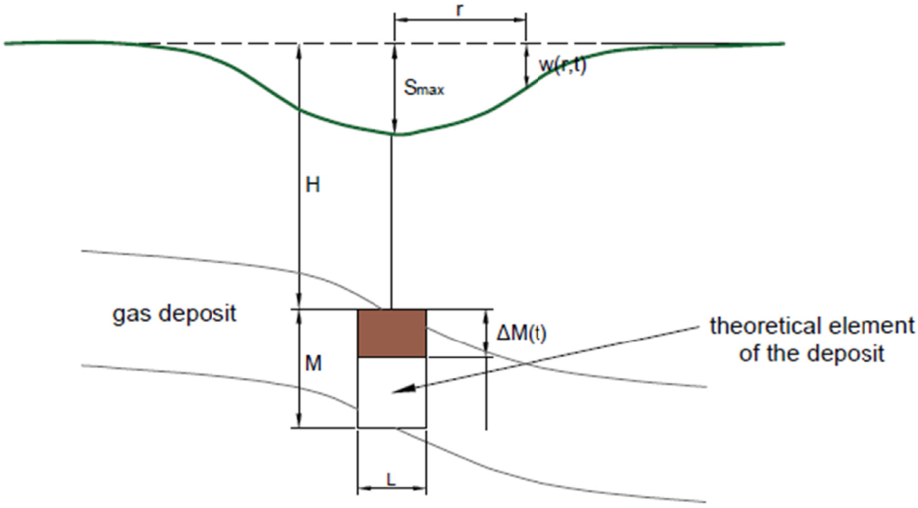

Fig. 5. Land subsidence forming above the exploitation of the *i*-element of the deposit

In the case of rock deposits such as sandstone with a porosity up to 20%, deposit compaction can be estimated using the Biot consolidation theory:

$$\Delta M_i(t) = C_{mi}\left[p_0 - p_i(t)\right]M_i \tag{14}$$

$$C_{mi} = \frac{\lambda_i(\eta)}{E_{si}} \tag{15}$$

where:

- C_{mi} – compaction ratio of the *i*-deposit element, being the vertical deformation of the deposit per unit pressure change,
- p_0 – initial pressure,
- $p_i(t)$ – pressure in the *i*-deposit element at time *t*,
- M_i – thickness of the porous deposit,
- E_{si} – rigidity module of the deposit rock formations,
- $\lambda_i(\eta)$ – Biot index depending on the type of deposit rock formation and its porosity.

The value of the compaction ratio depends on the type of rock formation and its deformation parameters. Literature often refers to the correlation between the value of the compaction ratio and porosity (Teeuw, 1973; Schutjens et al., 1995).

Figure 6 shows a comparison of the calculation and measured profile of the subsidence trough over the gas deposits in Groningen/Netherlands (Sroka, Schober, 1990).

4. Calculation of land surface raising in the process of mining water level increase

In the case of longwall cavern mining, a disintegrated rock mass area forms above the mined cavity. This zone is characterized by a relatively high porosity and thus high permeability and capacity as a water reservoir, created by the rising table of mining water. Increasing pressure in the pores of the disintegrated rock mass zone leads to its expansion and increase in volume. The change in volume capacity of the disintegrated zone may be described with formula:

$$K(t) = d_m \cdot \Delta p(t) \cdot \lambda \cdot M \cdot L^2 \tag{16}$$

where:

- λ – relative height of the disintegrated rock mass element (i.e. $\lambda = 3$ corresponds to an absolute height equal to three times the thickness of the mined deposit),

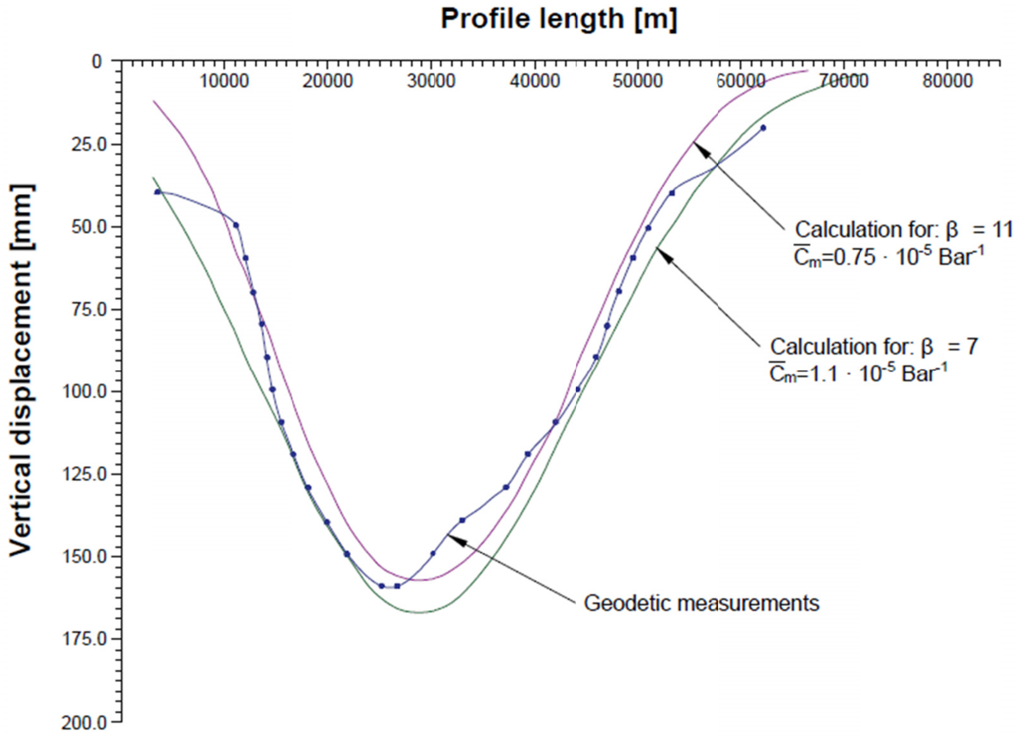

Fig. 6. Comparison of the measured and theoretically calculated subsidence trough for the Groningen gas deposit (status as of 1987)

$\Delta p(t)$ – porous pressure increase in the disintegrated rock mass area, depending on the water head over that area,

d_m – expansion coefficient; example values in Table 1.

Tab. 1. Experience to date concerning land surface rising caused by flooding of former hard coal mines (Graovski et al., 2013)

Mining zone / Literature	**Maximum depth [m]**	**Total thickness of selected deposit seams [m]**	**Maximum subsidence [m]**	**Maximum rising (uplifting) [cm]**	**Angle of main influence γ [gon]**	**$d_m \cdot \lambda$ [m²/MN]**	**Expansion index d_m [m²/MN]**	**Young modulus [MN/m²]**	**Calculation methods**
1	**2**	**3**	**4**	**5**	**6**	**7**	**8**	**9**	**10**
Zwickau [6]	1150	15	9	16			$0.24 \cdot 10^{-2}$	46.6	Fenk
Limburg [17]	1000	14	10	23		$1.40 \cdot 10^{-2}$	$\lambda = 4$; $0.35 \cdot 10^{-2}$		Pöttgens
Freital Bannewitz [27]	640	5	2.7	6.6		$1.44 \cdot 10^{-2}$	$\lambda = 4$; $0.36 \cdot 10^{-2}$		Pöttgens
Freital Gittersee [27]	280	5	2.46	2.8		$0.51 \cdot 10^{-2}$	$\lambda = 4$; $0.13 \cdot 10^{-2}$		Pöttgens
Freital Bannewitz [27]	640	5	2.67	6.6			$0.22 \cdot 10^{-2}$	45.91	Fenk
Freital Gittersee [27]	280	5	2.46	2.8			$0.12 \cdot 10^{-2}$	16.40	Fenk
Ibbenbüren Westfeld [12]	730	4.5	1.9	10.1		$1.44 \cdot 10^{-2}$	$\lambda = 3$; $0.46 \cdot 10^{-2}$		Pöttgens
Sophia-Jacoba [18]	790			25	12 gon	$1.06 \cdot 10^{-2}$	$\lambda = 4$; $0.26 \cdot 10^{-2}$		Sroka & Preuße
Königstein	260	18 Teilversatz	1.1	3.5	11 gon	$0.89 \cdot 10^{-2}$	$\lambda = 4$; $0.22 \cdot 10^{-2}$		Sroka & Preuße
Königstein	260	18 Teilversatz	1.1	3.5			$0.29 \cdot 10^{-2}$	6.68	Fenk
Königsborn*	1000	17.8	11.5	21.6	12 gon	$1.09 \cdot 10^{-2}$	$\lambda = 3$; $0.36 \cdot 10^{-2}$		Sroka & Preuße

(* – status as of 2015) Figures in [] brackets refer to the original publication)

As part of the research project contracted by the RAG Aktiengesellschaft coal company, Sroka and Preuβe have performed in 2012 a forecast of land uplifting for the Königsborn mine (eastern area of the Ruhr). Measurement results from 2015 (Fig. 7) after completion of the flooding procedure have confirmed at least qualitative compliance with the prognostic calculations made based on the Knothe theory (Sroka, 2005; Sroka, Preuße, 2009).

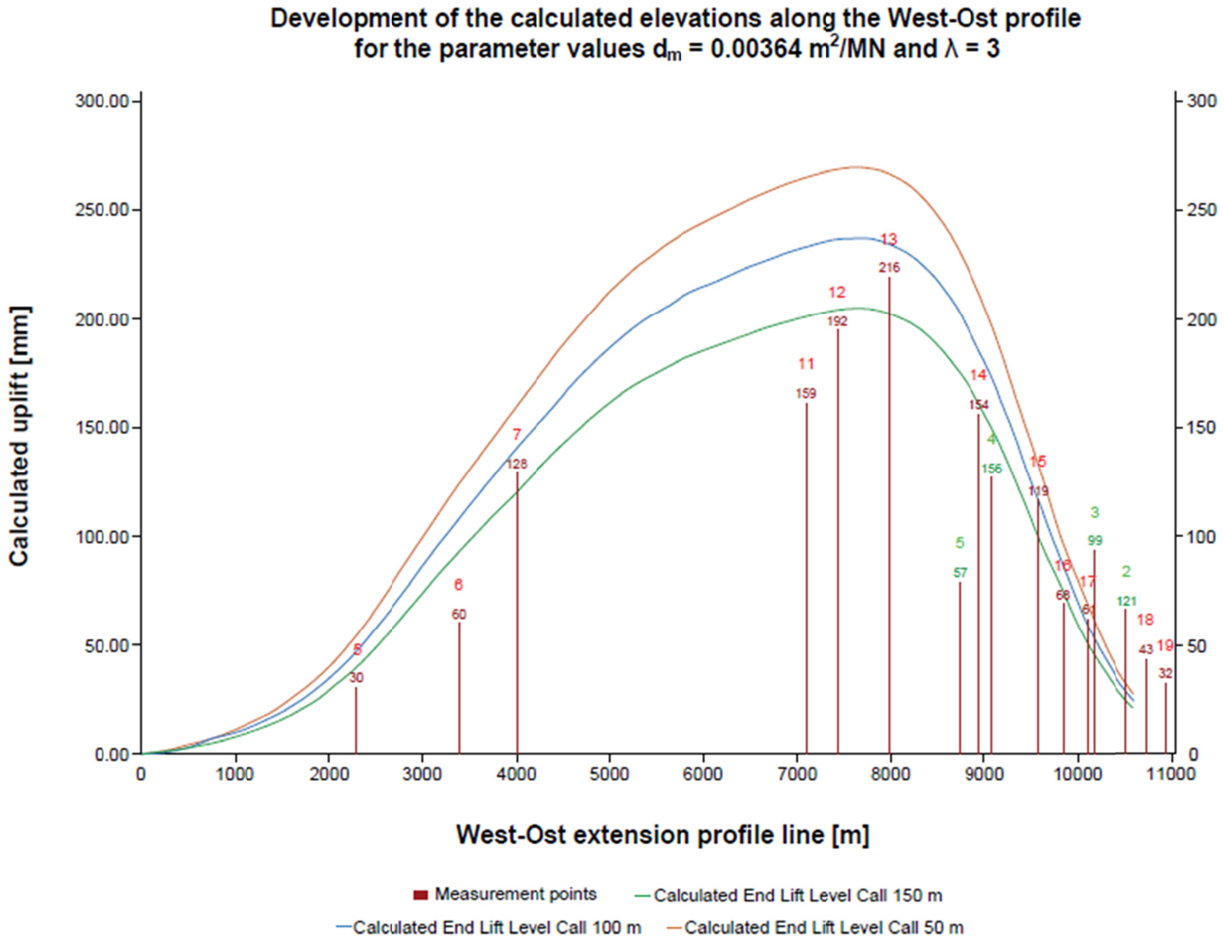

Fig. 7. Comparison of the calculated and measured uplifts in the Königsborn mine area (Sroka, Preuße, 2015)

5. Calculation of subsidence over tunnels

In 1952, professor Knothe has published a solution concerning forecasting of land subsidence for the first metro (subway) line project, to be built in Warsaw. This solution has also been presented in the sessions of the International Rock Mass Mechanics Office in place at that time, whose members included eminent scientists and engineers specializing in the domain of rock mass mechanics.

Later on, Peck (1969) and Schmidt (1974) have formulated a solution based on the same principle, i.e. the fundamental Gaussian function solution, in the form of the following formula (17):

$$s(x) = s_{max} \cdot \exp\left(-\frac{x^2}{2i^2}\right) = \frac{V_k}{i\sqrt{2\pi}} \exp\left(-\frac{x^2}{2i^2}\right) \tag{17}$$

where:

- x – distance of the calculation point from the axis of the tunnel,
- s_{max} – maximum subsidence over the axis of the tunnel,
- i – parameter of a value corresponding to the distance between the subsidence trough inflection point (in this point, subsidence rates reach approximately 0.6 s_{max}) and the axis of the tunnel,
- V_k – tunnel convergence volume per 1 m of its length [m^3/m].

The value of parameter *i* depends on the rock and ground condition of the layers on top of the tunnel. According to Schmidt (1974), for a rock mass formation, the value of this parameter can be calculated with formula (18):

$$i = \left(\frac{H}{2a}\right)^{\chi} \cdot a \tag{18}$$

for $0.8 \leq \chi \leq 1.0$.

Whereas according to Atkinson and Potts (1977), formula (19) and (20):

$$i = 0.25(H + a) \tag{19}$$

$$i = 0.25(1.5H + 0.5a) \tag{20}$$

where:

H – depth of the tunnel,

a – radius of a circular cross section tunnel.

The first formula is applicable to fine grain grounds (i.e. sand), medium compaction without additional load of the land surface and the second formula to compacted and pre-consolidated grounds with additional surface loading (Tajduś et al. 2016 and others).

Comparing the solution by Peck with the parametrisation defined by Knothe, we obtain a relationship between the parameter of impact range and parameter *i*: $r = \sqrt{2\pi} \cdot i$, leading to the following solution:

$$s(x) = s_{\max} \cdot \exp\left(-\pi \frac{x^2}{r^2}\right) \tag{21}$$

where:

$$s_{\max} = \frac{V_h}{r} \tag{22}$$

The solution related to the application of Knothe's theory in calculation of indexes of land deformation over tunnels in construction, in determination of permissible daily progress of drilling (related to the protection of land surface constructions) and in protection of land facilities and constructions using retainer walls is presented, among others, in the publications of Hörich, Sroka (2004), Tajduś et al. (2016) and Misa (2016).

6. Subsidence calculations in the case of deep geothermal installations

There are antennas of the German Centre of Aviation and Space (Deutsches Zentrum für Luft- und Raumfahrt e.V. (DLR)) near a planned geothermal installation. Further to the above, due to the great importance of those antennas, used among other things to plot position and coordinate movements of artificial satellites, the DLR has reported concerns related to the possible disturbance of antenna operation caused by the geothermal installation and more particularly by potential land subsidence.

The solutions and analyses presented by the authors (Sroka, Tajduś, 2011) being part of the expert review performed for that purpose, demonstrated that the vertical land surface displacements caused by deep geothermal operations may be caused by the following factors:

1. extraction of volumes,
2. increasing or decreasing pressure in the geothermal deposit, and
3. thermal contraction – lowing of the temperature of the geothermal reservoir rock formation and the resulting change in volume of the reservoir rock.

Analysing the planned production diagrams and the assumptions for the planned installations in Weilheim, approximately 40 km south from Munich it has been found that the first two factors have practically no impact on vertical displacement of land surface points. The production process assumes that the production and re-injection boreholes will be operated in a closed-circuit system, without extraction of volumes (water) from the geothermal reservoir. Also changes of pressure in the rock mass are relatively small and insignificant from perspective of possible land surface displacements. The project assumed that in the area of the production boreholes, pressure in the reservoir will drop by approximately 7 bars, whereas in the reinjection borehole area it will increase by approximately 12 bars.

Of the three factors listed, the remaining one is therefore the thermal contraction factor. The project assumes the over a period of 30-35 years, temperature of the reservoir rock formations will decrease by approximately 88°C. Decrease in temperature will lead to shrinking of rock volume in the geothermal reservoir and in consequence, among other things to the subsidence of the overlaying rock formations.

The Weilheim geothermal deposit is located in the Late Jurassic geological formation composed of limestone and dolomite rock formations. The deposit lays at a depth of 3050 m (top edge) and its thickness is of approximately 350 m. Design studies and simulation calculations allowed determination of the geometry of the reservoir in which the temperature will be decreasing. Calculations indicate that this geometry can be described with a cuboid with a square base (1028 × 1028 m) and height equal to the thickness of the reservoir (350 m). Calculations have also indicated that due to the cooling of the geothermal deposit, its height will decrease by approximately 250 mm. Table 2 shows results of calculations of the maximum subsidence and subsidence and inclination near the location of the closest antenna. The calculations were made for an impact range angle between 30° and 50°.

Tab. 2. Calculation results for maximum subsidence and subsidence and inclination in the AN1 antenna location, depending on the value of main impact range angle

β [°]	s_{max} [mm]	s_{AN1} [mm]	T_{AN1} [mm/m]
30	7.4	6.7	0.0013
35	10.7	9.1	0.0026
40	14.9	12.0	0.0047
45	20.3	15.1	0.0080
50	27.4	18.4	0.0132

Results of the land subsidence distribution and boundaries of the reservoir in which there will be a decrease in temperature are shown in Figure 8.

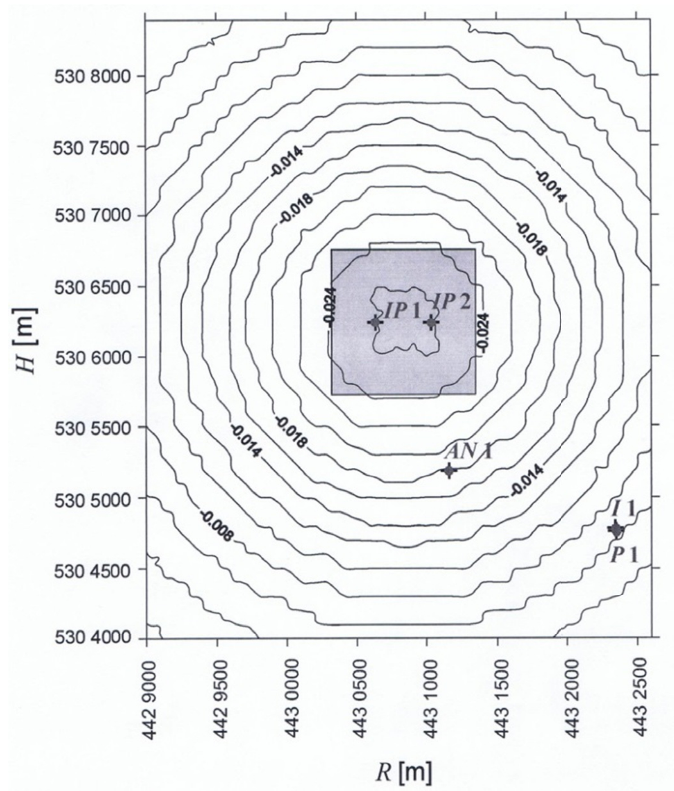

Fig. 8. Land surface subsidence in the area of the geothermal installation
(Legend: AN1 – nearest DLR antenna, I – reinjection boreholes, P – production boreholes)

The maximum value of inclination for the AN1 antenna location is T_A = 0.0132 mm/m = 0.76 m deg. This value is approximately ten times lower than the boundary value indicated by the DLR (threshold value requiring adjustment of the antenna's vertical alignment).

7. Application of the Knothe theory in modelling increase in vertical pressure

The introduction of high-yield longwalls in the Ruhr Coal Mining industry led to high risk levels in the longwall mining areas adjacent to active mining operations. This was caused by significant increases in exploitation pressure in the area of longwall mining front, which in turn led to significant convergence in the undercut mining drifts. In order to predict the exploitation pressure, theories of professor Knothe were used in calculation of the components of the deformation tensor in points located in the rock mass (Sroka, Schober, 1989).

Classic theory of elasticity indicates the following relationship between deformation of the rock mass caused by mining operations and the increase in vertical pressure:

$$\sigma_{zz} = \sigma_{33} = \lambda \cdot \theta + 2\mu \cdot \varepsilon_{33} \tag{23}$$

$$\theta = \sum_{i=1}^{i=3} \varepsilon_{ii} \tag{24}$$

where: λ, μ – Lame constants.

This model, as indicated by mining practice, allows a relatively accurate determination of the distributions of exploitation pressures and it is qualitatively compliant with the Everling-Meyer (1972) and te Kook (1989) models applied by the German mining industry. In comparison with these models, the model by Sroka, Schober (1989) is allowing simple consideration of the mining exploitation rate, having a significant influence on the value of deformation ε_{ii} (i=1-3), more particularly on the value of vertical deformation.

8. Conclusion

The conclusion from this report is that the current applications of the Knothe theory are much more extensive than its classical application in the mining of coal deposits. Knothe's theory is a versatile tool allowing formulation of simple and transparent solutions to many issues related to the calculation of subsidence and other deformations caused by extraction of volumes from the rock mass formations due to mining or post-mining activities.

References

Atkinson J., Potts M., 1977: *Ground movements near shallow model tunnels in sand*. Proceedings of large ground movement and settlement.

Everling G., Meyer A.G., 1972: *Ein Gebirgsdruckmodell als Planungshilfe*. Glückauf – Forschungshefte 33 (1972), Nr. 2.

Graovski A., Sroka A., Wedekind C., 2013: *Untersuchungen zu Auswirkungen an der Tagesoberfläche nach Einleitung der Flutung am Beispiel des Sanierungsstandortes Königstein der Wismut GmbH*. 14. Geokinematischer Tag, Freiberg 2013, Tagungsband p. 60-74.

Haupt W., Sroka A., Schober F., 1983: *Die Wirkung verschiedener Konvergenzmodelle für zylinderförmige Kavernen auf die übertägige Senkungsbewegung*. Das Markscheidewesen, 90 (1983), Heft 1, p. 159-164.

Hartmann A., 1984: *Ein Beitrag zur Überwachung von Kavernenanlagen*. Technische Universität Clausthal, Dissertation, 15. Juni 1984.

Hejmanowski R., Sroka A. et al., 2001: *Prognozowanie deformacji górotworu i powierzchni terenu na bazie uogólnionej teorii Knothego dla złóż stałych, ciekłych i gazowych*. Biblioteka Szkoły Eksploatacji Podziemnej. Wydawca IGSMiE PAN. Kraków. ISBN 83-87854-04-2.

Hengst G., 2014: *Monitoring der durch Kavernenkonvergenz induzierten Bodensenkungen unter Betrachtung ihrer Wirkungen auf die ökologischen Zusammenhänge*. 15. Geokinematischer Tag, 15. Und 16. Mai 2014. Freiberg.

Hörich S., Sroka A. 2004: *Vorausberechnung der Bodenbewegungselemente über Tunnelbauten im Lockergebirge*. Proceedings of XII International Congress of International Society for Mine Surveying. Fuxin-Beijing, China, 20-26 September, 2004, p. 528-531.

Knothe S., 1951: *Wpływ podziemnej eksploatacji na powierzchnię z punktu widzenia zabezpieczenia położonych na niej obiektów*. Praca doktorska. AGH Kraków.

Knothe S., 1953: *Równanie profilu ostatecznie wykształconej niecki osiadania*. Archiwum Górnictwa, Tom 1, zeszyt 1, PWN Warszawa, p. 22-38.

Leitzke C., Sroka A., 1987: *Indirekte Überwachung unzugänglicher Speicher- und Deponiekavernen*. Kali u. Steinsalz Bd. 9 (1987), Heft 10, p. 334-344.

Misa R., 2016: *Metody ograniczenia wpływu eksploatacji podziemnej na obiekty budowlane poprzez zastosowanie rozwiązań geotechnicznych*. Wydawnictwo IMG PAN. ISBN 978-83-946392-0-4.

Peck R.B., 1969: *Deep excavations and tunneling in soft ground*. 7th International Conference on Soil Mechanics and Foundation Engineering. State of Art Volume: 7, Issue: 3, Pages: 225-290, Mexico.

Schmidt BV., 1974: *Prediction of Settlement due to Tunneling in Soil: Three case Histories*. Rapid Excavation and Tunneling Conference, San Francisco, California, June, p. 1974-1999.

Schober F., Sroka A., 1987: *Zur Langzeitbelastung über- und untertägiger Anlagen bei Speicher- und Deponiekavernen*. Kali u. Steinsalz Bd. 9 (1987), Heft 12, p. 408-414.

Schutjens P.M.T.M., Fens T.W., Smits R.M.M., 1995: *Experimental observations of the unixial compaction of quartz-rich reservoir rock at stress of up to 80 MPa*. Land Subsidence, Balkema, Rotterdam.

Sroka A., Schober F., 1982: *Die Berechnung der maximalen Bodenbewegungen über kavernenartigen Hohlräumen unter Berücksichtigung der Hohlraumgeometrie*. Kali u. Steinsalz Bd. 8 (1982), Heft 8, p. 273-277.

Sroka A., 1984: *Abschätzung einiger zeitlicher Prozesse im Gebirge. Schriftenreihe Lagerstättenerfassung und -darstellung, Bodenbewegungen und Bergschäden, Ingenieurvermessung*. Kolloquium Leoben 15/16.11.1984, p. 103-132.

Sroka A., Schober F., Sroka T., 1987: *Ogólne zależności między wybraną objętością pustki poeksploatacyjnej a objętością niecki osiadania z uwzględnieniem funkcji czasu*. Ochrona Terenów Górniczych, nr 79/1, Katowice, p. 3-9.

Sroka A., Schober F., Bartosik-Sroka T., 1988: *Vorausberechnung von Gebirgsbewegungen bei geneigten flözartigen Lagerstätten unter Berücksichtigung anisotroper Gebirgseigenschaften und des zeitlichen Konvergenz- und Verzögerungsverhaltens des Gebirges*. Abschlussbericht zum DFG –Forschungsvorhaben Ha 526/15-1, Clausthal – Zellerfeld.

Sroka A., Schober F., 1989: *Die mathematische Modellbildung als Mittel bergmännischer Planung*. Das Markscheidewesen 96 (1989), Nr. 4, p. 331-334.

Sroka A., Schober F., 1990: *Studie zur Analyse und Vorhersage der Bodensenkungen und des Kompaktionsverhaltens des Erdgasfeldes Groningen/Emsmündung (unveröffentlicht)*. Clausthal-Zellerfeld, Mai 1990.

Sroka A., 2005: *Ein Beitrag zur Vorausberechnung der durch den Grubenwasseranstieg bedingten Hebungen*. 5. Altbergbau--Kolloquium, TU Clausthal 2005, Tagungsband, p. 453-462.

Sroka A., Preuße A., 2009: *Zur Prognose flutungsbedingter Hebungen*. 9.Altbergbau-Kolloquium, Montanuniversität Leoben 2009. Tagungsband, p. 184-196.

Sroka A., Tajduś K., 2011: *Stellungnahme zu den möglichen Senkungen infolge des Betriebes der geplanten Geothermieanlage im Westen von Weilhem (Bereich Lichtenau).* Ekspertyza na zlecenie firmy Erdwärme Oberland GmbH w Monachium. Drezno, 04-08.2011.

Sroka A., Preuße A., 2015: *Schlussbericht zum Forschungsvorhaben „Risiken durch Grubenwasseranstieg"*. FE-Nr.: 0760 0000, RAG Aktiengesellschaft, Herne (unveröffentlicht).

Tajduś K., Misa R., Sroka A., 2016: *Metody określania zmian deformacji górotworu i powierzchni terenu w rejonie drążonego tunelu*. Prace Instytutu Mechaniki Górotworu PAN, Tom 18, nr 4, p. 63-72.

Sroka A., Misa R., Tajduś K., Klaus M., Meyer S., Feldhaus B., 2017: *Forecast of rock mass and ground surface movements caused by the convergence of salt caverns for storage of liquid and gaseous energy carriers*. 18. Geokinematischer Tag. 11. und 12. Mai 2017 in Freiberg. Wagner Digitaldruck und Medien GmbH. Heft 2017 -1, p. 34-51.

Teeuw D., 1973: *Laboratory Measurment of Compaction Properties of Groningen Reservoir Rock*. Verhandeligen kon. Ned. Geol. Mijnbouwk. Gen. Volume 28.

te Kook J., 1989: *Ermittlung des Gebirgsdruckes aus gemessenen Gebirgsbewegungen*. Glückauf-Forschungshefte 50 (1989), Nr. 1.